Korean J. of Chem. Eng., **8**(2), 73-79 (1991)

MASS TRANSFER IN LIQUID-FLUIDIZED AND SPOUTED BEDS OF ION EXCHANGE RESIN AT LOW REYNOLDS NUMBER

Seung Jai Kim, Chan Yong Chung, Sung Yong Cho* and Rok Ju Chang**

Department of Chemical Engineering, Chonnam National University,
300 Yongbong-dong, Buk-ku, Kwangju 500-757, Korea
*Catalysis and Separation Process Lab., KIST, Seoul
**Hankook Shell Oil Co., Kwangju Office

(Received 11 September 1990 • accepted 16 April 1991)

Abstract—Rates of mass transfer from the liquid phase to small ion exchange resin particles (0.78 mm in mean diameter) in fluidized and spouted beds were studied experimentally. Dilute aqueous solution of sodium hydroxide was fed into the beds of strong cation exchange resin and the exit concentration of the solution was determined by conductivity measurement. In spouted beds, the initial conversion and K_L increased with bed height, but decreased with fluid flowrate. The model, applying material balance of the reactant and axisymmetric flow of fluid in the annulus of a spouted bed, predictions of the initial conversion in spouted beds are satisfactory. In fluidized beds, the obtained mass transfer coefficients were correlated and compared with other works.

INTRODUCTION

Fluid-particle mass transfer in fixed beds, fluidized beds and bubble columns has been studied extensively since it is important for the design and development of such fluid-particle contactors [1-5]. In most of these works, the obtained experimental data have been correlated in terms of dimensionless groups [1]. For the liquid-particle systems, the mass transfer rate has been measured for the dissolution of solid particles, adsorption and ion exchange.

Several types of ion exchangers such as bubble columns, fluidized beds and packed beds have been widely used in chemical and biochemical processes [3]. For the design of such exchangers, the basic information for the flow and fluid-particle mass transfer is required. Ion exchange operations are not always easy with packed bed exchangers because of the possible blockage of resins and channeling in the bed. The types of beds with mobile resins can eliminate these problems and lead to increase in an ion exchange efficiency.

Dwivedi and Upadhay [1] proposed generalized correlations for the fluid-particle mass transfer coefficient for fixed and fluidized beds. Based on the analysis of various experimental data, they concluded that the Chilton-Colburn J_d factor is inversely proportional to the bed voidage. Recently, Prakash et al. [5] reported that the Dwivedi-Upadhay correlation can be adapted to gas-liquid-solid three phase systems and proposed a new correlation.

Hadzismajlovic et al. [3] studied mass transfer in a spout-fluid bed. The authors proposed a model for calculating the initial conversion and obtained an empirical correlation for the overall mass transfer coefficient, and suggested that the fluid-spouted bed will be useful for treating solutions contaminated with suspended solid particles which would lower the specific capacities of fixed bed ion exchangers.

In this work, the mass transfer rate of Na^+ ion from aqueous solution of NaOH to resin particles was measured in fluidized and spouted beds. The mass transfer coefficients obtained were correlated and compared with earlier works. In spouted beds, the experimental data were used to verify the model.

EXPERIMENTAL

Fig. 1 shows a schematic diagram of experimental setup. The beds used for the experiment were made of transparent acrylic resin and 60 mm in inside diameter. The fluidized bed has a lower section, 150 mm in height, which is packed with 0.71 mm glass particles. The spouted bed has a flat base and a jet inlet

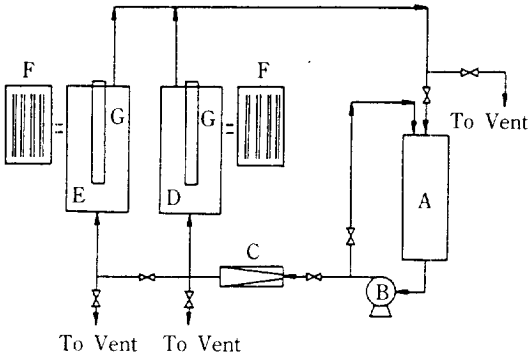

A-Reactant tank B-Pump
C-Flowmeter D-Spouted bed
E-Fluidized bed F-Piezometer tube plate
G-Electric conductivity meter

Fig. 1. Schematic diagram of experimental setup; A: reactant tank, B: pump, C: flowmeter, D: spouted bed, E: fluidized bed, F: piezometer tube plate, G: electric conductivity meter.

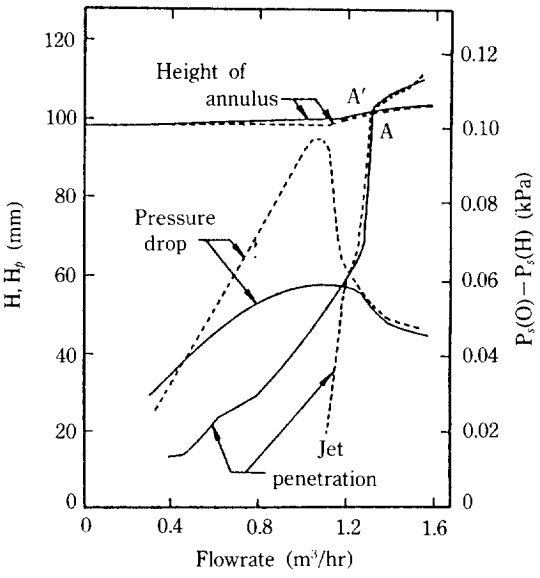

Fig. 2. Bed pressure drop, annulus height, jet penetration and spout fountain height as a function of fluid flowrate; ----: increasing flowrate, —: decreasing flowrate.

5 mm in inside diameter. The spout diameter and fluid streamline were measured at the flat wall of a half-cylindrical spouted bed of the same size. The ion exchange resin, Amberlyst-15, was sieved in swollen state on standard sieves and the fluid temperature was kept at 23± 0.5℃.

For the spouting experiment, a measured quantity of resin, 0.78 mm in mean diameter, was placed in the bed and distilled water was used as a spouting medium. The bed pressure drop, annulus height, jet penetration and spout fountain height are shown in Fig. 2 as a function of flowrate. The bed is shallow enough for the jet to penetrate it. With increasing fluid flowrate the jet begins to penetrate the bed, and as the flowrate is increased, penetration continues rapidly with decreasing bed pressure drop until the jet reaches the top of the bed at point the A'. On decreasing flowrate from above the minimum spouting, the jet ceases to penetrate the top of the bed at point the A. This flowrate, seen in Fig. 2, is defined as the minimum spouting flowrate, U_{ms}, ΔP_{ms} is the measured pressure drop, $P_s(O)-P_s(H)$, along the axis of the symmetry in the minimum spouting condition.

Above a certain bed height, the jet does not penetrate to the top of the bed regardless of the flowrate, because the bed expands faster than the jet can penetrate it [6]. The criterion for determining H_m and $(U_{ms})_{Hm}$ for these beds are formulated by observing the change in the shape of the jet with decreasing flowrate. As the fluid velocity is lowered from above

Table 1. Experimentally measured minimum spouting properties; D_c=60 mm, d_i=5 mm, ρ_p=1300 kg/m^3

H(mm)	U_{ms} (mm/s)	d_s (mm)	ΔP_{ms} (Pa)	ΔP_{mf} (Pa)
35	0.54	7.5	21.5	72.4
50	0.76	8.0	37.2	98.8
65	0.90	8.6	65.6	135.0
80	1.04	9.4	84.1	165.3
98	1.28	10.5	104.7	195.6
120	1.42	11.7	139.9	229.8
140	1.50	12.7	171.2	264.1
165*	1.58	13.5	198.5	294.4

*: H_m

$(U_{ms})_{Hm}$, the jet narrows at the top, finally assuming a flame tip shape. $(U_{ms})_{Hm}$ is the highest fluid velocity for which the flame tip-shape jet is visible. The height of the spout to the tip of the flame shape jet at $(U_{ms})_{Hm}$ is denoted H_m. $(\Delta P_{ms})_{Hm}$ is spout pressure drop at $(U_{ms})_{Hm}$ in the bed of height, H_m.

The fluid streakline and residence time were measured by using a dye tracer technique. Methylene blue solution, 1% by weight, was injected into the annulus, the streakline was photographed and the residence time along the streamline was measured. The spout diameter listed in Table 1 is the mean value.

For the mass transfer experiment, aqueous solution of sodium hydroxide, 0.06 mol/L, was pumped through

the beds of ion exchange resin, metered by a set of rotameters. The effluent concentration of the solution was determined by conductivity measurement (Solution Analyzer, Cole-Parmer Instrument, Model: 5800-05). Experiments were performed varying the amount of resin in the bed and fluid flowrate.

MASS TRANSFER COEFFICIENT AND HYDRODYNAMIC MODEL

The overall mass transfer coefficient was calculated from Eq. (1).

$$K_L = V/S \ \ln \frac{C_i - C^*}{C_e - C^*} \tag{1}$$

where V is volumetric fluid flowrate and S is the surface area of ion exchange resin in the bed.

The material balance in a spouted bed, proposed by Mathur and Lim [7], was applied for the reactant. The schematic is shown in Fig. 3.

In the spout, the material balance of the reactant gives

$$U_s A_s C_s = [U_s A_s + d(U_s A_s)](C_s + dC_s) + \pi d_s dz U_r C_s + K_{Ls} dS_s C_s \tag{2}$$

where $U_r = -\frac{1}{\pi d_s} \frac{d(U_s A_s)}{dz}$ (3)

$$S_s = \frac{6A_s(1-\varepsilon_s)}{d_p} z \tag{4}$$

Substituting Eqs. (3) and (4) into Eq. (2), we obtain

$$U_s \frac{dC_s}{dz} + 6(1-\varepsilon_s) \ K_{Ls} \frac{C_s}{d_p} = 0 \tag{5}$$

where U_s, C_s and ε_s are the fluid velocity, reactant concentration and voidage in the spout, respectively.

In the annulus, the material balance of the reactant gives

$$U_a A_a C_a + \pi U_r d_s dz C_s = K_{La} dS_a C_a + [U_a A_a + d(U_a A_a)](C_a + dC_a) \tag{6}$$

where $U_r = \frac{1}{\pi d_s} \frac{d(U_a A_a)}{dz}$ (7)

$$S_a = \frac{6A_a(1-\varepsilon_a)}{d_p} z \tag{8}$$

Substituting Eqs. (7) and (8) into Eq. (6), we obtain

$$U_a \frac{dC_a}{dz} + \frac{1}{A_a} \frac{d(U_a A_a)}{dz} (C_a - C_s) + \frac{6(1-\varepsilon_a) K_{La} C_a}{d_p} = 0 \tag{9}$$

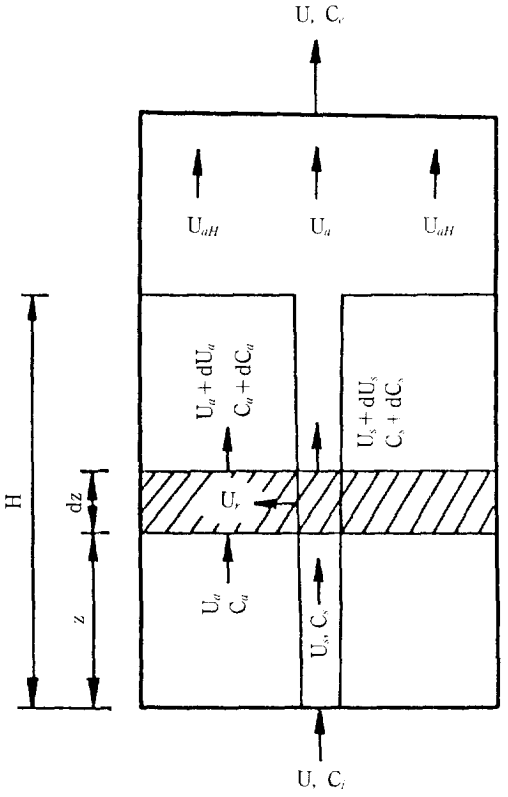

Fig. 3. Two-region model of a spouted bed reactor.

where U_a, A_a, C_a and ε_a are the fluid velocity, cross sectional area, reactant concentration and voidage in the annulus, respectively. The boundary conditions for Eqs. (5) and (9) are

$$z = 0, \ C_a = C_s = C_i \tag{10}$$

For the spouting of fine particles with liquid, Darcy's law is applicable in the annulus since the fluid inertial force term in the Ergun equation is less than 10% of the pressure drop term, so that the basic field equations and boundary conditions are the same as those of Lefroy and Davidson [8] except for the spout-annulus interfacial boundary condition. The spout-annulus interfacial boundary condition [Eq. (11)] was obtained experimentally since none of the equation proposed for coarse particles fits our experimental data well. Based on those data, p (r_s, z) was represented in terms of a third degree polynomial:

$$p(r_s, z) = P_s(z) - P_s(H) = \Delta P_s(a + by + cy^2 + dy^3) \tag{11}$$

where a, b, c and d are constants. For the axisymmetric motion about the z axis of a cylinder, the streamfunction in the annulus can be expressed as

$$\psi(r, z) = -\frac{\Delta P_s}{f_1} r \frac{I_1(mr)K_1(mr_s) - I_1(mr_s)K_1(mr)}{I_0(mr_s)K_1(mr_s) + I_1(mr_s)K_0(mr_s)} \times \sum_{n=1,3,5}' \frac{C_n}{n} \sin(n\pi z/2H) \quad (12)$$

where $C_n = \left\{ -\frac{8b}{n^2\pi^2} - \frac{32}{n^3\pi^3}(c+3d) \right\} \sin(n\pi/2) + \frac{192d}{n^4\pi^4}$

The details of the development of Eq. (12) can be found in Kim [9]. The voidage in the annulus, ε_a, was assumed to be equal to ε_{mf}. The voidage in the spout, ε_s, was calculated from Lefroy and Davidson theory based on the Ergun friction factor [10].

Eqs. (5) and (9) were solved numerically using U_a and U_s calculated from Eq. (12) and material balance of the fluid. Effluent concentration of the reactant was calculated from Eq. (13):

$$C_e = (V_{aH}C_{aH} + V_{sH}C_{sH})/V \quad (13)$$

The degree of conversion was defined as

$$X_A = 1 - C_e/C_i \quad (14)$$

RESULTS AND DISCUSSION

1. Hydrodynamics

Hydrodynamic experiments in fluidized and spouted beds were done with distilled water. U_{mf} and ε_{mf} measured in the fluidized bed are 1.3 mm/s and 0.41, respectively. The spouted bed properties in a bed of height equal to or less than H_m at minimum spouting are listed in Table 1. At $U = U_{ms}$ and $H = H_m$, $\Delta P_s = 0.674\Delta P_{mf}$. When the bed height is less than or equal to H_m, the bed pressure drop data at $U = U_{ms}$ can be correlated as

$$\Delta P_{ms}/(\Delta P_{ms})_{Hm} = 1.13h - 0.13 \quad (\text{for } h > 0.2) \quad (15)$$

with the correlation coefficient of 0.96.

The axial pressure profile in the spout was measured and correlated by Eq. (16) with the correlation coefficient of 0.97:

$$\frac{P_s(z) - P_s(H)}{\Delta P_s} = 1.00 - 0.25y - 1.11y^2 + 0.36y^3 \quad (16)$$

Using the data in Table 1, the axial pressure profile in the spout and Eq. (12), the fluid velocity in the annulus was calculated and compared with predictions from other flow models. Fig. 4 shows the comparison of the various flow models at $H = H_m$. In the Grbavcic et al. [11] and Lefroy and Davidson [8] models, U_a at H_m is equal to U_{mf}. The one dimensional model of Grbavcic et al. [11] predicts rapid increase in U_a in the lower section of the bed. Piccinini, Grace and Mathur [12] modified Grbavcic et al.'s relationship with U_a at H_m which is 0.88 U_{mf}. The axisymmetric flow model of this study assuming Darcy flow in the annulus predicts U_a at H_m is 0.70 U_{mf} as shown in Fig. 4. As the bed height is decreased below H_m, U_a is decreased further and U_a at $H = 0.39$ H_m is 0.41 U_{mf}.

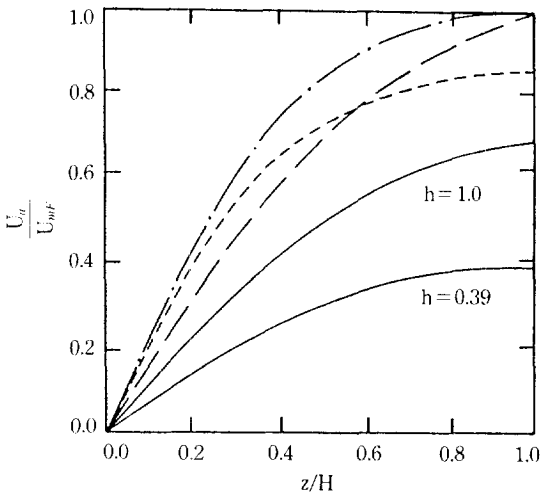

Fig. 4. Comparison of models predicting average fluid velocity in the annulus at $U = U_{ms}$; ----: Piccinini et al.'s model [12], - -: Lefroy and Davidson model [8], -·-: Grbavcic et al.'s model [11], —: axisymmetric model (this work).

The fluid streamline and velocity calculated from the axisymmetric flow model, Eq. (12), represent the measured ones very well for $Re < 5$. However, one dimensional flow models predict streamlines which are practically plug flow and do not represent the experimentally measured fluid streaklines.

The bed voidage variation in the fluidized bed with fluid velocity was measured. The values calculated from Richardson and Zaki's correlation [13] were slightly lower than the experimental values of this study, however, the correlation predicted our data reasonably well.

2. Mass Transfer

Experimental breakthrough curves for fluidized and spouted beds are shown in Fig. 5 as a function of fluid flowrate. In each of the beds, a known amount of resin was poured into the column with the static bed of height 60 mm. As can be seen in Fig. 5, C_e/C_i in the spouted bed is substantially higher than that in the fluidized bed at the same fluid flowrate and reaction time, and the difference becomes larger for higher

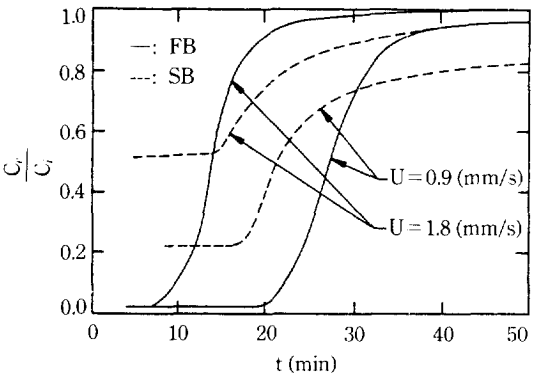

Fig. 5. Breakthrough curves in fluidized and spouted beds; D_c=60 mm, H_0=65 mm, C_i=0.06 mol/L.

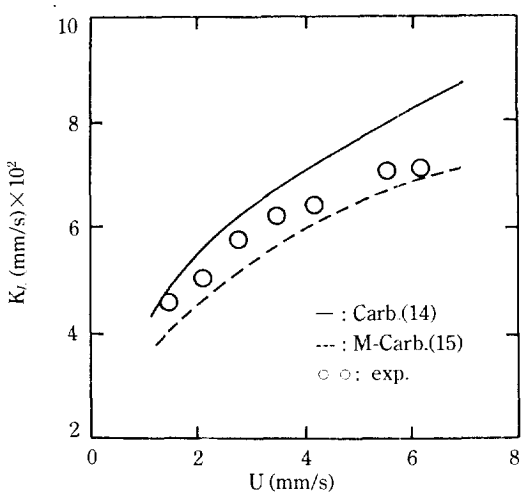

Fig. 6. Comparison of K_L values in fluidized bed; D_c=60 mm, d_p=0.78 mm, C_i=0.06 mol/L.

flowrates. This is obviously due to the difference in the fluid flow pattern between the two beds. In spouted beds, a substantial amount of fluid flows through the spout where the voidage and fluid velocity are high. And furthermore, as the fluid flowrate is increased above the minimum spouting, the portion of the fluid flowing through the spout is also increased.

The values of K_L were calculated from Eq. (1) in the initial period of the experiment and the results in fluidized beds are shown in Fig. 6. The figure shows that the experimental values of this study are located in between the calculated ones from Carberry's [14] and Mixon and Carberry's [15] equations.

In Table 2, the experimental values of Sh are given together with the values calculated from the correlations in the literature [1, 15, 16]. In the calculation of

Table 2. Comparison of correlations for predicting Sh in fluidized beds; d_p=0.78 mm, D=0.00193 mm²/s, Sc=508.8. ε was calculated from Richardson and Zaki correlation [13]

U (mm/s)	Re	Sh (exp't)	Sh (Eq. 17)	Sh (Eq. 18)	Sh (Eq. 20)	Sh (Eq. 21)
1.4	1.11	12.43	13.34	18.43	24.63	12.33
2.1	1.67	13.52	14.35	19.91	24.36	14.19
2.8	2.22	15.74	16.98	21.11	24.18	15.60
3.5	2.78	16.80	18.35	22.05	24.06	16.96
4.2	3.34	17.08	19.53	22.79	23.92	18.05
5.6	4.45	19.02	21.60	24.16	23.77	19.96
6.3	5.00	19.10	22.50	24.72	23.71	20.79

Sh, the diffusivity coefficient for NaOH in water, D=0.00193 mm²/s, was taken from Harriot [16].

Mixon and Carberry [15] and Snowdon and Turner [17] developed Eq. (17) and Eq. (18), respectively. Although they proposed these

$$Sh = 0.974\ Re^{0.5} Sc^{1/3} \varepsilon^{0.5} \quad (17)$$

$$Sh = 0.81\ Re^{0.5} Sc^{1/3} \varepsilon^{1} \quad (18)$$

equations for similar experimental conditions in fluidized beds, the effect of bed voidage on Sh is very different.

Dwivedi and Upadhyay [1] proposed a generalized correlation for mass transfer coefficients in terms of the Chilton-Colburn mass transfer factor based on the regression of various liquid-phase data:

$$\varepsilon J_d = 1.1068\ Re^{-0.72} \quad (\text{for } Re<10) \quad (19)$$

This equation can be rewritten as

$$Sh = 1.1068\ Re^{0.28} Sc^{0.33} \varepsilon^{-1} \quad (\text{for } Re<10) \quad (20)$$

Eq. (20) shows that the effect of Re on Sh is smaller while that of ε on Sh is greater compared to Eq. (17). In the range of this study, Table 2 shows that Eq. (20) predicts better as Re decreases, but this equation gives values which are practically constant and too high for all Re. Although Dwivedi and Upadhyay [1] showed that their general correlation could predict the liquid-phase data in the fixed and fluidized beds with average deviation of 23.45%, some data they used for the correlation were different by the factor of almost 6 in the extreme case. This shows that there are uncertainties in the application of the general correlation to a specific experimental condition. Snowdon and Turner's correlation, Eq. (18), also does not represent our data well obviously due to the difference in the effect of bed voidage.

Although Mixon and Carberry's correlation, Eq.

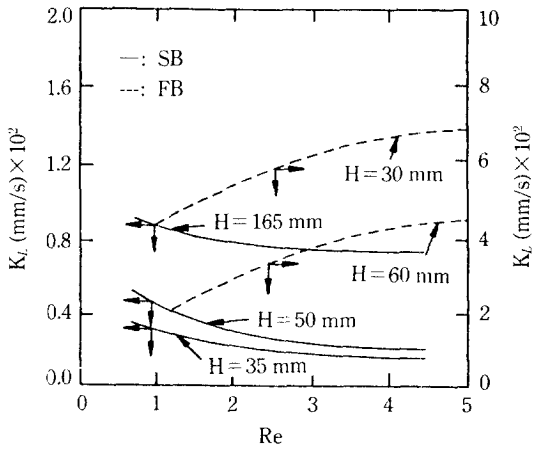

Fig. 7. Comparison of K_L in fluidized and spouted beds; D_c=60 mm, C_i=0.06 mol/L.

(17), represents our experimental data relatively well, substantial improvements can be made by changing the coefficient in Eq. (17) from 0.974 to 0.90.

$$Sh = 0.90\ Re^{0.5}Sc^{0.33}\varepsilon^{-0.5} \quad (\text{for } 1<Re<5) \qquad (21)$$

Eq. (21) correlates our experimental data in Table 2, with the correlation coefficient of 0.96.

In order to compare K_L values in fluidized and spouted beds, K_L is plotted in Fig. 7 as a function of Re. One can see from the figure that K_L in fluidized beds is always greater than that in spouted beds for the same fluid velocity and bed height, and the differences are increased as the bed height and fluid velocity are increased. The effect of flowrate on K_L is also different between the two beds. In fluidized beds, K_L increases with Re, while it decreases with Re in spouted beds.

Using the axisymmetric flow model assuming Darcy flow in the annulus and Eqs. (5) and (9), the values of exit concentration in the spout and annulus were calculated, and then the overall exit concentration was obtained. As shown in Table 3, the axisymmetric flow model predicts overall conversion quite well. One dimensional flow model of Grbavcic et al. [11], Eq. (22), was also used to predict the overall conversion. The fluid velocity calculated from Eq. (22) is

$$U_{aH} = U_{mf}[1-(1-h)^3] \qquad (22)$$

This velocity is substantially higher than that from the axisymmetric flow model of this study as shown in Fig. 4. For the same spout inlet fluid flowrate, V, V_{sH} decreases as V_{aH} increases. Since C_{aH} in spouted beds is always smaller than C_{sH}, C, calculated from Eq. (13) based on the one dimensional flow model,

Table 3. Comparison of experimental and calculated values of Xe in spouted beds; C_i=0.06 mol/L

H(mm)	35	50	65	165
U(mm/s)	0.54	0.76	0.90	1.58
d_s(mm)	7.5	8.0	8.6	13.5
U_{aH}(mm/s)	0.21	0.35	0.49	0.90
ε_a	0.414	0.420	0.422	0.430
ε_s	0.80	0.76	0.74	0.68
K_{Ls}(mm/s)	0.118	0.117	0.113	0.108
K_{La}(mm/s)	0.025	0.026	0.030	0.042
C_{sH}(mol/L)	0.046	0.038	0.030	0.0022
C_{aH}(mol/L)	0.0026	0.0021	0.0014	0.0001
C_e(mol/L)	0.0300	0.0218	0.0148	0.0011
X_e(axi)	0.512	0.634	0.753	0.980
X_e(1D)	0.951	0.946	0.957	0.990
X_e(exp't)	0.567	0.713	0.795	0.986

To Vent To Vent To Vent

Eq. (22), is much lower than that from the axisymmetric flow model. This is the reason why the degree of the overall conversion calculated from Eq. (14) based on the one dimensional flow model is much higher than that from the axisymmetric flow model as shown in Table 3.

CONCLUSIONS

The following conclusions are drawn from the present work.

1. The initial conversion and K_L in fluidized beds are always greater than those in spouted beds for the same fluid velocity, but the differences are decreased as the bed height is increased.

2. As Re is increased, K_L is increased in fluidized beds while it is decreased in spouted beds.

3. In fluidized beds, the experimental K_L values can be correlated as $Sh = 0.9\ Re^{0.5}Sc^{0.33}\varepsilon^{-0.5}$ with correlation coefficient of 0.96.

4. In spouted beds, Mathur and Lim's material balance with an axisymmetric flow model predicts the initial conversion reasonably well.

ACKNOWLEDGEMENT

The authors wish to acknowledge a grant-in-aid for research from the KOSEF.

NOMENCLATURE

A_a : $(\pi/4)(D_c^2-d_s^2)$ [mm²]
A_s : $(\pi/4)d_s^2$ [mm²]

C_a : reactant concentration in the annulus [mol/L]
C_i : inlet concentration of reactant [mol/L]
C_e : effluent concentration of reactant [mol/L]
C^* : equilibrium concentration of reactant [mol/L]
C_s : reactant concentration in the spout [mol/L]
D : diffusivity coefficient [mm^2/s]
d_p : particle diameter [mm]
d_s : spout diameter [mm]
f_1 : $150[(1-\varepsilon)^2/\varepsilon^3][\mu/d_p^2]$ [kg/mm^3s]
H : bed height [mm]
h : H/H_m [−]
H_m : maximum spoutable bed height in the condition of minimum spouting [mm]
H_0 : static bed height [mm]
H_p : jet penetration or spout fountain height [mm]
I_0 : modified Bessel function (1st kind, order zero) [−]
I_1 : modified Bessel function (1st kind, order one) [−]
J_d : mass transfer factor; $(K_L/U)Sc^{2/3}$ [−]
K_0 : modified Bessel function (2nd kind, order zero) [−]
K_1 : modified Bessel function (2nd kind, order one) [−]
K_L : mass transfer coefficient [mm/s]
m : $\pi/2H$ [mm^{-1}]
P_s : dynamic fluid pressure in the spout [Pa]
ΔP_s : $P_s(z)-P_s(H)$ [Pa]
r : distance from the vertical axis of symmetry of the column [mm]
r_c : column radius [mm]
r_s : spout radius [mm]
Re : Reynolds number ($U\, d_p\, \rho/\mu$) [−]
S : surface area of ion exchange resin [mm^2]
Sc : Schmidt number ($\mu/\rho D$) [−]
Sh : Sherwood number ($K_L\, d_p/D$) [−]
U : superficial fluid velocity in axial direction [mm/s]
V : fluid flowrate in the bed [mm^3/s]
y : z/H [−]
z : vertical distance from the spout inlet [mm]
ε : voidage [−]
ρ_f : fluid density [kg/m^3]
ρ_p : particle density [kg/m^3]
ψ : stream function [mm^3/s]

Subscripts

a : in the annulus
H : at z=H
H_m : at $H=H_m$
mf : in the minimum fluidization
ms : in the minimum spouting condition
s : in the spout

REFERENCES

1. Dwivedi, P. and Upadhyay, N.: *Ind. Chem. Process Des. Dev.*, **16**, 157 (1977).
2. Goto, S. and Matsumoto, Y.: Proceedings of the Asian Conf. on Fluidized Bed and Three Phase Reactors, p. 520, Tokyo, Japan, Dec. 14-17 (1988).
3. Hadzismajlovic, D. E., Vukovic, D. V., Zdanski, F. K., Grbavcic, Z. B. and Littman, H.: *Chem. Eng. J.*, **17**, 227 (1979).
4. Koloini, M., Sopcic, M. and Zumer, M.: *Chem. Eng. Sci.*, **32**, 637 (1977).
5. Prakash, A., Briens, C. L. and Bergougnou, M. A.: *Can. J. Chem. Eng.*, **65**, 228 (1987).
6. Kim, S. J. and Littman, H.: *Can. J. Chem. Eng.*, **65**, 723 (1987).
7. Mathur, K. B. and Lim, C. J.: *Chem. Eng. Sci.*, **29**, 789 (1974).
8. Lefroy, G. A. and Davidson, J. F.: *Trans. Instn. Chem. Engrs.*, **47**, T120 (1960).
9. Kim, S. J.: *Kor. J. Chem. Eng.*, **1**, 35 (1984).
10. Day, J. Y., Morgan, M. H. and Littman, H.: *Chem. Eng. Sci.*, **42**, 1461 (1987).
11. Grbavcic, Z. B., Vukovic, D. V., Zdanski, F. K. and Littman, H.: *Can. J. Chem. Eng.*, **54**, 33 (1976).
12. Piccinini, N., Grace, J. R. and Mathur, K. B.: *Chem. Eng. Sci.*, **34**, 1257 (1979).
13. Richardson, J. F. and Zaki, W. N.: *Trans. Instn. Chem. Engrs.*, **32**, 35 (1954).
14. Carberry, J. J.: *AIChE J.*, **6**, 460 (1960).
15. Mixon, F. O. and Carberry, J. J.: *Chem. Eng. Sci.*, **13**, 30 (1960).
16. Harriot, P.: *AIChE J.*, **8**, 93 (1962).
17. Snowdon, C. B. and Turner, J. C. R.: Proc. Int. Symp. of Fluidization, Einhoven Univ. Press, Amsterdam (1967).